Maximal- and minimal-height distributions of fluctuating interfaces

T. J. Oliveira and F. D. A. Aarão Reis
Instituto de Física, Universidade Federal Fluminense, Avenida Litorânea s/n, 24210-340 Niterói RJ, Brazil
(Received 12 November 2007; published 15 April 2008)

Maximal- and minimal-height distributions (MAHD, MIHD) of two-dimensional interfaces grown with the nonlinear equations of Kardar-Parisi-Zhang (KPZ, second order) and of Villain-Lai-Das Sarma (VLDS, fourth order) are shown to be different. Two universal curves may be MAHD or MIHD of each class depending on the sign of the relevant nonlinear term, which is confirmed by results of several lattice models in the KPZ and VLDS classes. The difference between MAHD and MIDH is connected with the asymmetry of the local height distribution. A simple, exactly solvable deposition-erosion model is introduced to illustrate this feature. The average extremal heights scale with the same exponent of the average roughness. In contrast to other correlated systems, generalized Gumbel distributions do not fit those MAHD and MIHD, nor those of Edwards-Wilkinson growth.

DOI: 10.1103/PhysRevE.77.041605 PACS number(s): 81.15.Aa, 68.35.Ct, 05.40.−a, 68.55.J−

I. INTRODUCTION

Extreme value statistics (EVS) was already used in several fields of science and engineering [1,2] and has recent important applications in surface and interface science. For instance, it is relevant for modeling the evolution of corrosion damage because a material failure may occur when the size of the deepest pit attains a critical value [3].

In uncorrelated random variable sets where the probability density functions (PDF) decrease faster than a power law, a universal normalized distribution of extreme values is obtained. It is usually called Gumbel's first asymptotic distribution [1,4], $g(x;n)$, which gives the probability density of the nth extreme value of that set (normalized by the average extreme value) lying in the range $[x,x+dx]$. However, in several physical systems where correlations are present, it was observed that fluctuations of some global quantities could be fit by generalized Gumbel distributions [5–7], i.e., the first asymptotic distribution with noninteger n values. This was explained by the connections between the EVS of correlated variables and sums of independent variables drawn from exponential PDF [8]. It shows that Gumbel statistics goes far beyond the description of uncorrelated variables sets.

EVS was already studied analytically and numerically in one-dimensional models of fluctuating interfaces [9–11], showing differences from uncorrelated statistics. In two-dimensional Edwards-Wilkinson (EW) interfaces (Brownian curves), a fit of the maximal-height distributions (MAHD) by a Gumbel curve was suggested [7], although the analytical form of the tail of the EW MAHD is not the same as the Gumbel curves. A common feature of those works was to consider Gaussian interfaces with up-down reflection symmetry [9–11]. However, several real and model interfaces do not possess this symmetry [12]. Important examples are the nonlinear growth models of Kardar-Parisi-Zhang (KPZ) [13] and of Villain-Lai-Das Sarma (VLDS) [14], which have many applications to real interfaces [15–17]. Height distributions (measured relatively to the average) of those systems are asymmetric, i.e., the interfaces may be dominated by sharp peaks and flat valleys or vice versa. This raises the question whether MAHD and minimum-height distributions (MIHD) are the same in these systems. Recent work on persistence in VLDS growth [18] also motivates this study because the different exponents for positive and negative height persistence may be a consequence of that asymmetry.

Besides the comparison of MAHD and MIHD in those models, recent works on EVS of fluctuating interfaces suggest additional (and not less important) questions. The first one is connected with the possibility of fitting their extreme height distributions (EHD) by generalized Gumbel distributions, since there is numerical evidence in the recent literature that this is possible for some correlated variable sets, the work of Bertin [8] illustrating this possibility with exactly solvable models. The second question is the scaling of the average maximal height, since EW interfaces showed an unanticipated scaling as the square of the average roughness [7]. It contrasts with several one-dimensional interfaces, where average maximal height and average roughness scale in the same way. This scaling is important to correlate the extreme events (sharpest peaks or deepest valleys) with the evolution of surface roughness.

The aim of this paper is to address those questions by performing a numerical study of the MAHD and MIHD in the steady states of the KPZ and VLDS equations and of various lattice models belonging to those classes in $2+1$ dimensions, which is the most relevant case for applications. The numerical approach for KPZ and VLDS growth is necessary because no analytical calculation of related quantities are known in $d=2$. We will show that, for each growth class, two universal scaled distributions are obtained, which may be a MAHD or a MIHD depending on the sign of the coefficient of the relevant nonlinear term (second order in KPZ, fourth order in VLDS). In order to highlight the effects that asymmetric PDF (i.e., asymmetric distributions of local heights) may have on MAHD and MIHD, we will discuss their differences in a random deposition-erosion model on an inert flat substrate. Furthermore, we will show that average maximal and minimal heights is all those models scale as the average roughness, thus EW in $d=2$ is an exception [7]. Finally, we will show that MIHD and MAHD of KPZ, VLDS, and EW classes in $d=2$ cannot be fit by generalized

Gumbel distributions, despite reasonable fits of the peaks are possible.

The rest of this work is organized as follows. In Sec. II we analyze the features of MAHD and MIHD of the nonlinear interface growth models. In Sec. III, we show the differences between MAHD and MIHD in a simple exactly solvable model. In Sec. IV we analyze the scaling of the average maximal and minimal heights and compare MAHD and MIHD with Gumbel curves. In Sec. V we summarize our results and present our conclusions.

II. MAHD AND MIHD OF NONLINEAR INTERFACE GROWTH MODELS

The KPZ equation

$$\frac{\partial h}{\partial t} = \nu_2 \nabla^2 h + \lambda_2 (\nabla h)^2 + \eta(\vec{x},t) \tag{1}$$

was proposed in 1986 as a hydrodynamic description of interface growth [13]. In Eq. (1), h is the interface height at position $\vec{x}$ and time t, the linear term represents the effect of surface tension, the nonlinear term accounts for an excess velocity due to local slopes and η is a Gaussian noise with zero mean and covariance $\langle \eta(\vec{x},t)\eta(\vec{x}',t')\rangle = D\delta^d(\vec{x}-\vec{x}')\delta(t-t')$, where D is constant and d is the dimension of the substrate.

We integrated the KPZ equation in $d=2$ with a simple Euler method, as shown in Ref. [19], with the scheme for suppression of instabilities of Ref. [20]. We used the coupling constant $g \equiv \lambda_2^2 D/\nu_2^3 = 24$ and time increment $\Delta t = 0.04$, in discretized boxes with spatial step $\Delta x = 1$ and linear sizes $8 \le L \le 64$.

We also simulated three discrete KPZ models (i.e., models which are described by the KPZ equation in the continuum limit) in sizes $32 \le L \le 256$: the restricted solid-on-solid (RSOS) model [21], the ballistic deposition (BD) [22], and the etching model of Mello *et al.* [23] (the deposition and aggregation rules of those models can be found in the above references and/or Ref. [12]). From inspection of their growth rules, one knows that $\lambda_2 > 0$ for BD and the etching model and $\lambda_2 < 0$ for the RSOS model (see, e.g., the arguments in Ref. [24]).

For each model and each lattice size, distributions with at least 10^7 different configurations were obtained to ensure high accuracy, which is particularly important at their tails. The extremes were calculated relatively to the average height of each configuration, the minima being absolute values of the differences from the average.

Figure 1(a) shows the difference between scaled MAHD and MIHD of the KPZ equation in box size $L=64$. There, $P(m)dm$ is the probability that the extreme lies in the range $[m, m+dm]$, $x \equiv (m - \langle m \rangle)/\sigma$ and $\sigma \equiv (\langle m^2 \rangle - \langle m \rangle^2)^{1/2}$. Curves for smaller box sizes coincide with those in Fig. 1(a), showing that the difference between MAHD and MIHD is not a consequence of finite-size effects.

In Fig. 1(b), we compare those scaled distributions with MAHD and MIHD of the discrete KPZ models. The MIHD of the KPZ equation collapses with the MIHD of the etching model and with the MAHD of the RSOS model. The plot also shows the MAHD of the KPZ equation shifted down in the vertical direction, which collapses with the shifted MAHD of BD and MIHD of the RSOS model. Thus, MAHD (MIHD) of models with $\lambda_2 > 0$ are equal to MIHD (MAHD) of models with $\lambda_2 < 0$, which defines two universal EHD for the KPZ class.

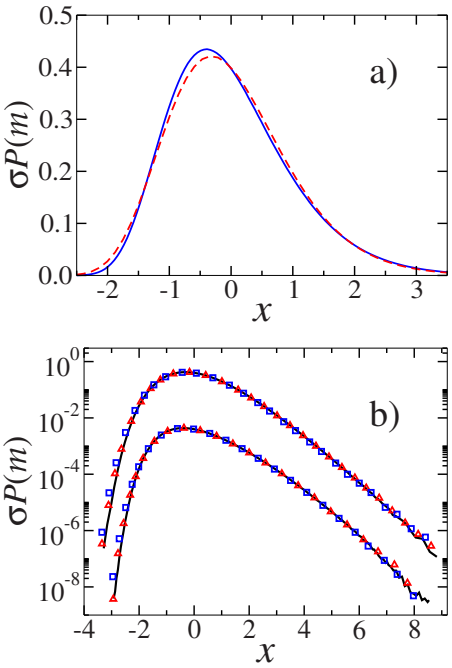

FIG. 1. (Color online) (a) Scaled MAHD (solid curve) and MIHD (dashed curve) of the KPZ equation in box size $L=64$. (b) Upper curves: scaled MIHD of the KPZ equation (solid curve) and etching model (triangles), and MAHD of the RSOS model (squares). Lower curves: scaled MAHD of the KPZ equation (solid curve) and BD (triangles), and MIHD of the RSOS model (squares), shifted by two decades in the vertical direction. Box size is $L=64$ for KPZ equation and $L=256$ for discrete models.

Estimates of skewness and kurtosis of those EHD quantitatively confirm the visual agreement in Fig. 1(b). The skewnesses of the EHD are shown in Figs. 2(a) and 2(b) as a function of $1/L^{1/2}$. The small finite-size dependence of the

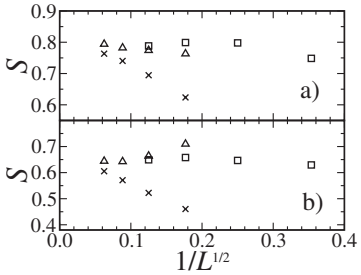

FIG. 2. (a) Finite-size dependence of the skewness S of (a) MAHD of the KPZ equation (squares) and etching model (triangles), and MIHD of the RSOS model (crosses); (b) MIHD of the KPZ equation (squares) and etching model (triangles), and MAHD of the RSOS model (crosses). The variable in the abscissa was chosen to make clearer the evolution of the data as $L \to \infty$. BD data were not shown because they superimpose the etching model data.

data for the KPZ equation, BD, and the etching models leads to an estimate $S \approx 0.79$ for $(\lambda_2 > 0)$ MAHD and $(\lambda_2 < 0)$ MIHD [Fig. 2(a)]. For $(\lambda_2 > 0)$ MIHD and $(\lambda_2 < 0)$ MAHD, we obtain $S \approx 0.65$ [Fig. 2(b)]. Surprisingly, the largest finite-size effects are observed in the RSOS data, which uses to be the best discrete KPZ model for numerical study of roughness scaling [27]. This is probably a consequence of discretization of the very smooth surfaces of RSOS deposits.

A consequence of the difference between MAHD and MIHD is the possibility to use them to identify the sign of the coefficient of the nonlinear term in cases where it is not known *a priori*. Certainly this demands an accurate calculation of the MAHD and MIHD because the scaled curves of Fig. 1(a) are very close to each other. This is frequently possible with computer models, but probably very hard with typical experimental data. Anyway, at this point EVS is superior to the scaling of the local height distributions (the PDF), since the latter are usually distorted by huge finite-size effects [27]. For instance, the asymmetry of the height distributions of BD in sizes $L \lesssim 500$ incorrectly suggests $\lambda_2 < 0$ for that model [27].

We also observe that the right tails of MAHD and MIHD of the KPZ class tend to simple exponentials for large m. Thus, these tails differ from the tails of the KPZ roughness distributions, which are stretched exponentials [28].

Now we analyze the EHD of the VLDS equation

$$\frac{\partial h}{\partial t} = -\nu_4 \nabla^4 h + \lambda_4 \nabla^2 (\nabla h)^2 + \eta(\vec{x}, t), \tag{2}$$

which was originally proposed for molecular beam epitaxy. This equation was integrated with $\nu_4 = 1$, $\lambda_4 = 1$, $D = 1/2$, and $\Delta t = 0.01$, using the same methods applied to the KPZ equation, in sizes $8 \leq L \leq 32$. We also simulated a generalized conserved RSOS model (CRSOS) [25,26], which belongs to the VLDS class, in sizes $16 \leq L \leq 128$ (growth rules of this model are given in Ref. [26]).

MAHD and MIHD are also different in the VLDS class, as shown in Fig. 3(a). The MAHD has skewness $S \approx 0.63$ and there is negligible difference between the scaled curves for $L = 16$ [not shown in Fig. 3(a)] and $L = 32$. The right tails of the MIHDs show small finite-size effects [Fig. 3(a)], but the distance from the MAHD increases with L. This indicates that MAHD and MIHD are also different in this class. As $L \to \infty$, we estimate $S \approx 0.55$ for the MIHD, as shown in Fig. 3(b). Also note that both EHD have Gaussian-shaped right tails [$\propto \exp(-m^2)$].

On the other hand, MAHD and MIHD of the CRSOS model have non-negligible finite-size effects. Extrapolation of the skewnesses of EHD of the CRSOS model in finite-size lattices are also shown in Fig. 3(b). They suggest that MAHD and MIHD of both models are asymptotically the same. From the symmetry of the VLDS equation, it means that $\lambda_4 > 0$ for the CRSOS model, similarly to its one-dimensional original version, which is exactly solvable [29].

III. MAHD AND MIHD OF AN EXACTLY SOLVABLE MODEL

In order to highlight the difference between MAHD and MIHD and its relation to the height distribution, we consider

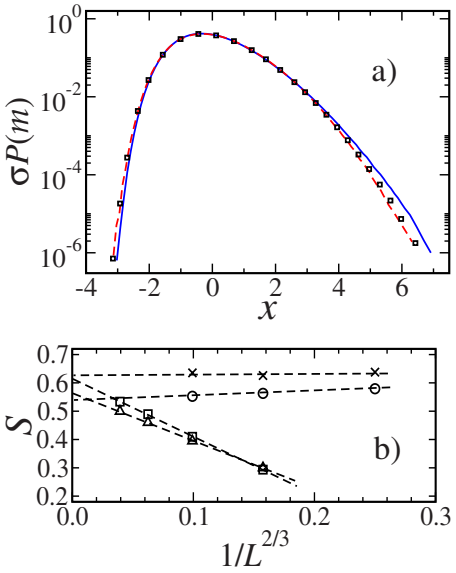

FIG. 3. (Color online) (a) Scaled MAHD in $L = 32$ (solid curve) and MIHD in $L = 32$ (dashed curve) and $L = 16$ (squares) of the VLDS equation. (b) Finite-size dependence of the skewness S of EHD of the VLDS equation (crosses for MAHD, circles for MIHD) and of the CRSOS model (squares for MAHD, triangles for MIHD). The variable $1/L^{2/3}$ provides the best linear fits of the data (dashed lines).

an exactly solvable model of random deposition and erosion with an inert flat substrate at height $h = 0$, in the erosion-dominated regime. In this model, $q > 1/2$ is the probability of single-particle erosion $(h \to h-1)$ and $1-q$ of deposition $(h \to h+1)$, but erosion is possible only if $h > 0$.

The model corresponds to a random walk with a reflecting wall at $h = 0$. In the steady state, the probability of height h, $P(h)$, obeys

$$P(h) = qP(h+1) + (1-q)P(h-1), \quad h \geq 1, \tag{3}$$

and

$$P(0) = qP(1) + qP(0). \tag{4}$$

This gives the PDF

$$P(h) = \left(\frac{2q-1}{q}\right)\left(\frac{1-q}{q}\right)^h, \tag{5}$$

with average height $\langle h \rangle = \frac{1-q}{2q-1}$ above the substrate. In the limit $q \to 1/2$, we have $P(h) = \frac{1}{\langle h \rangle} \exp(-h/\langle h \rangle)$ with large $\langle h \rangle$.

Now consider that one measures the extremes in a set of L (independent) columns. At this point, it is important to observe that extremes must be measured relative to the average height $\langle h \rangle$, similarly to the other interface models. Thus, maximal heights are maximal values of $h - \langle h \rangle$ and minimum heights are maximal values of $\langle h \rangle - h$.

Concerning the MAHD, the conditions of applicability of Gumbel's first asymptotic distribution are satisfied, thus scaled MAHD is $g(x, 1)$ (explicit form given below).

Concerning the MIHD, we observe that the minimum absolute height is typically at the substrate $(h = 0)$ if L is large, i.e., it is highly probable to have at least one column with

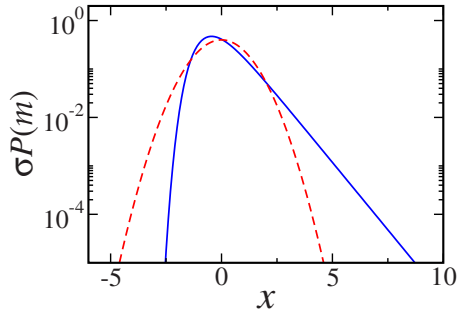

FIG. 4. (Color online) Scaled MAHD (solid curve) and MIHD (dashed curve) of the random deposition-erosion model in the erosion-dominated regime.

$h=0$ in the erosion-dominated regime. Thus the relative minimum is the average height of the L columns, $\bar{h}_L$, and the MIHD is the distribution of those values (of course, the ensemble average of $\bar{h}_L$ is $\langle h \rangle$). Since all columns are uncorrelated, fluctuations in $\bar{h}_L$ are Gaussian and the variance is L times smaller than the variance of the PDF, $\Delta \equiv \langle h^2 \rangle - \langle h \rangle^2 = \frac{q(1-q)}{(2q-1)^2}$. The probability of an absolute minimum m is proportional to $\exp[-(m-\langle h \rangle)^2/(2\Delta/L)]$, and so is the MIHD.

The difference between the scaled MAHD and MIHD is easily confirmed by visual inspection of the plots shown in Fig. 4. Gumbel's first asymptotic distribution shown there is given by

$$g(x;n) = \omega \exp(-n[e^{-b(x+s)} + b(x+s)]), \tag{6}$$

where $b = \sqrt{\psi'(n)}$, $s = [\ln n - \psi(n)]/b$ and $\omega = n^n b/\Gamma(n)$, with $\Gamma(x)$ the Gamma function and $\psi(x) = \partial \ln \Gamma(x)/\partial x$ [5,7].

The local height distribution (PDF) of this deposition-erosion model is highly asymmetric, with skewness $S_{PDF} = \frac{1}{\sqrt{q(1-q)}}$, so that $S_{PDF} \to 2$ as $q \to 1/2$. It contrasts with the slight asymmetry of KPZ ($S_{PDF} \approx 0.26$ [27]) and VLDS ($S_{PDF} \approx 0.20$ [25]) classes. Thus, comparison of Figs. 1(a), 3(a), and 4 strongly suggests that the difference between MAHD and MIHD is connected with the asymmetry of the height distribution.

IV. AVERAGE EXTREMAL HEIGHTS AND COMPARISON WITH GUMBEL DISTRIBUTIONS

We assume that the average values of extremes of KPZ and VLDS interfaces, $\langle m \rangle$, scale as

$$\langle m \rangle \sim L^{\alpha_m}. \tag{7}$$

The average roughness W scales with the roughness exponent α. We estimate α_m by extrapolation of effective exponents

$$\alpha_m(L) \equiv \frac{\ln[\langle m \rangle(L)/\langle m \rangle(L/2)]}{\ln 2}, \tag{8}$$

similarly to the procedure usually adopted to calculate the roughness exponent (see, e.g., Ref. [27]). Accurate calculation of α is usually performed with results of the discrete models instead of the growth equations, thus here we will also follow this procedure.

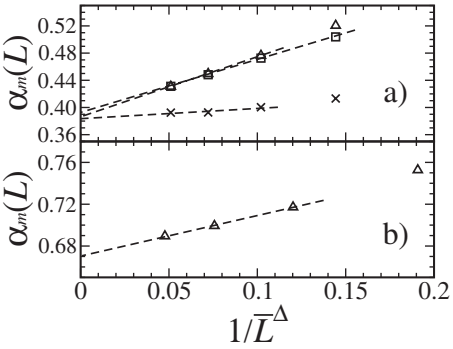

FIG. 5. Effective exponents $\alpha_m(L)$ of discrete models: (a) KPZ class (BD, crosses; etching, triangles; RSOS, squares) and (b) VLDS class (CRSOS model). $\bar{L}$ is the average size among L and $L/2$. The variables in the abscissa provide the best linear fits (dashed lines) with exponents $\Delta = 1/2$ (a) and $\Delta = 2/3$ (b).

Figures 5(a) and 5(b) show $\alpha_m(L)$ versus $1/L$ for the KPZ and VLDS models, respectively, obtained with the average maximal heights. The estimates of α_m are consistent with the best known estimates of the roughness exponents $\alpha \approx 0.39$ (KPZ) [27] and $\alpha \approx 0.67$ (VLDS) [25]. Results obtained with the average minimal heights are similar to those of Figs. 5(a) and 5(b). The fact that average values of extremes scale as the average roughness in the KPZ and VLDS classes in 2+1 dimensions suggests that the roughness can be used as an estimate of the order of magnitude of extremal height fluctuations. This feature may be important to foresight extremal fluctuations from roughness data.

However, this result contrasts with EW growth, where $\langle m \rangle$ scales as the squared roughness [7] (which we also confirmed by simulation). In Ref. [7], it is shown that uncorrelated Gaussian fluctuations with roughness scaling as $W \sim \sqrt{\ln L}$ (which is the case of EW in $d=2$) also lead to $\langle m \rangle \sim W^2$. Thus, the EW scaling of $\langle m \rangle$ may be related to a weaker influence of correlations when compared to other growth processes. Anyway, similar argument does not work for EW in $d=1$, thus we believe that it should not be considered a full explanation of the distinct EW scaling.

Now we compare the EHD of the nonlinear growth models with Gumbel curves [Eq. (6)]. This comparison is also performed with data for the EW equation (KPZ with $\lambda_2 = 0$), which was integrated with $\nu_2/D = 3$ and $\Delta t = 0.01$ in box sizes $8 \le L \le 64$.

In Fig. 6, we show the MAHD of the growth models and Gumbel curves with the same skewnesses: 0.79 for KPZ (Gumbel with $n=1.95$), 0.63 for VLDS ($n=2.90$), and 0.68 for EW ($n=2.60$). In all cases, the Gumbel curves provide reasonable fits of their peaks in log-linear plots, but the discrepancies in the tails are clear. Similar discrepancies are found in comparisons with MIHD of KPZ and VLDS classes. Thus, despite the wide applicability of Gumbel statistics to correlated systems, it is not able to represent the EVS of important interface growth processes in two-dimensional substrates, including the linear EW growth.

Finally, it is also interesting to note the right tail of the MAHD for EW growth, shown in Fig. 6, has a Gaussian

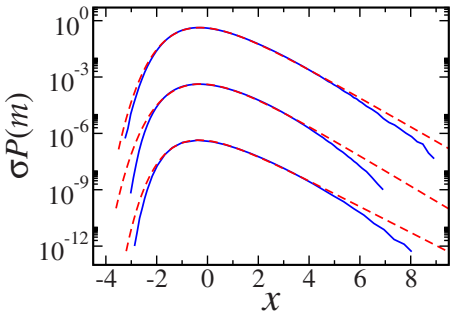

FIG. 6. (Color online) Scaled MAHD of the growth equations (solid curves) and Gumbel distributions with the same skewnesses (dashed curves): EW (compared with $n=2.6$), VLDS (shifted by three decades in vertical direction, compared with $n=2.9$), and KPZ (shifted by six decades, $n=1.95$).

shape [$\propto\exp(-m^2)$], which confirms the analytical prediction by Lee [7].

V. CONCLUSION

We showed that interface growth models with asymmetric local height distributions have different maximal and minimal height distributions, the most important examples being the KPZ and the VLDS classes in two dimensions. In each class, a pair of universal curves may be maximal or minimal height distributions depending on the sign of the relevant nonlinear term. The average maximal and minimal heights of KPZ and VLDS models scale as the average roughness, in contrast to the EW class. All extreme height distributions of interface growth models, including the linear EW model, cannot be fit by generalized Gumbel distributions.

Although the statistical analysis of interfaces use to focus on height distributions and/or roughness scaling [12], recent studies show that the statistics of global quantities are very useful to characterize them [2]. The EVS has the same advantages of roughness distribution scaling for this task, such as weak finite-size effects, but also reveals the sign of the nonlinear terms if sufficiently accurate date is available. Despite the fact that MAHD and MIHD of the KPZ and VLDS classes are rather similar and probably difficult to distinguish with experimental data, this is not always the case. For instance, in Fig. 4 we note that the distributions for the deposition-erosion model are very different. Thus we expect that the present work motivates experimental comparisons of MAHD and MIHD.

Information on rare events is also essential in systems where drastic changes in the dynamics occur if the global minima or maxima attain certain values, such as in corrosion damage. Finally, we believe that the present work also motivates additional studies of distributions of local extremes, which may be important for some applications (e.g., friction and parallel computing) [30].

ACKNOWLEDGMENTS

T.J.O. acknowledges support from CNPq and F.D.A.A.R. acknowledges support from CNPq and FAPERJ (Brazilian agencies).

[1] E. J. Gumbel, *Statistics of Extremes* (Columbia University Press, New York, 1958).
[2] S. T. Bramwell, P. C. W. Holdsworth, and J.-F. Pinton, Nature (London) **396**, 552 (1998); J. P. Bouchaud and M. Mézard, J. Phys. A **30**, 7997 (1997); R. W. Katz, M. B. Parlange, and P. Naveau, Adv. Water Resour. **25**, 1287 (2002); S. Moulinet, A. Rosso, W. Krauth, and E. Rolley, Phys. Rev. E **69**, 035103(R) (2004); J. F. Eichner, J. W. Kantelhardt, A. Bunde, and S. Havlin, *ibid.* **73**, 016130 (2006); S. Redner and M. R. Petersen, *ibid.* **74**, 061114 (2006).
[3] G. Engelhardt and D. D. Macdonald, Corros. Sci. **46**, 2755 (2004).
[4] R. A. Fisher and L. A. Tippett, Proc. Cambridge Philos. Soc. **24**, 180 (1928).
[5] S. T. Bramwell, K. Christensen, J.-Y. Fortin, P. C. W. Holdsworth, H. J. Jensen, S. Lise, J. M. López, M. Nicodemi, J.-F. Pinton, and M. Sellitto, Phys. Rev. Lett. **84**, 3744 (2000).
[6] T. Antal, M. Droz, G. Györgyi, and Z. Rácz, Phys. Rev. Lett. **87**, 240601 (2001).
[7] D.-S. Lee, Phys. Rev. Lett. **95**, 150601 (2005).
[8] E. Bertin, Phys. Rev. Lett. **95**, 170601 (2005); E. Bertin and M. Clusel, J. Phys. A **39**, 7607 (2006).
[9] S. Raychaudhuri, M. Cranston, C. Przybyla, and Y. Shapir, Phys. Rev. Lett. **87**, 136101 (2001).
[10] S. N. Majumdar and A. Comtet, Phys. Rev. Lett. **92**, 225501 (2004); J. Stat. Phys. **119**, 777 (2005).
[11] G. Györgyi, P. C. W. Holdsworth, B. Portelli, and Z. Rácz, Phys. Rev. E **68**, 056116 (2003); G. Schehr and S. N. Majumdar, *ibid.* **73**, 056103 (2006); G. Györgyi, N. R. Moloney, K. Ozogány, and Z. Rácz, *ibid.* **75**, 021123 (2007).
[12] A. L. Barabási and H. E. Stanley, *Fractal Concepts in Surface Growth* (Cambridge University Press, Cambridge, England, 1995).
[13] M. Kardar, G. Parisi, and Y.-C. Zhang, Phys. Rev. Lett. **56**, 889 (1986).
[14] J. Villain, J. Phys. I **1**, 19 (1991); Z.-W. Lai and S. Das Sarma, Phys. Rev. Lett. **66**, 2348 (1991).
[15] J. Krim and G. Palasantzas, Int. J. Mod. Phys. B **9**, 599 (1995).
[16] R. Paniago, R. Forrest, P. C. Chow, S. C. Moss, S. S. P. Parkin, and D. Cookson, Phys. Rev. B **56**, 13442 (1997); M. C. Salvadori, M. G. Silveira, and M. Cattani, Phys. Rev. E **58**, 6814 (1998); M. U. Kleinke, J. Davalos, C. Polo da Fonseca, and A. Gorenstein, Appl. Phys. Lett. **74**, 1683 (1999); P. L. Schilardi, O. Azzaroni, R. C. Salvarezza, and A. J. Arvia, Phys. Rev. B **59**, 4638 (1999); A. E. Lita and J. E. Sanchez, Jr., *ibid.* **61** 7692 (2000); D. Tsamouras, G. Palasantzas, and J. T. M. de Hosson, Appl. Phys. Lett. **79**, 1801 (2001).
[17] Y.-L. He, H.-N. Yang, T.-M. Lu, and G.-C. Wang, Phys. Rev. Lett. **69**, 3770 (1992); C. Thompson, G. Palasantzas, Y. P.

Feng, S. K. Sinha, and J. Krim, Phys. Rev. B **49**, 4902 (1994); D. C. Law, L. Li, M. J. Begarney, and R. F. Hicks, J. Appl. Phys. **88**, 508 (2000).

[18] M. Constantin, C. Dasgupta, P. Punyindu Chatraphorn, S. N. Majumdar, and S. Das Sarma, Phys. Rev. E **69**, 061608 (2004).

[19] K. Moser, J. Kertész, and D. E. Wolf, Physica A **178**, 215 (1991).

[20] C. Dasgupta, J. M. Kim, M. Dutta, and S. Das Sarma, Phys. Rev. E **55**, 2235 (1997).

[21] J. M. Kim and J. M. Kosterlitz, Phys. Rev. Lett. **62**, 2289 (1989).

[22] M. J. Vold, J. Phys. Chem. **63**, 1608 (1959).

[23] B. A. Mello, A. S. Chaves, and F. A. Oliveira, Phys. Rev. E **63**, 041113 (2001).

[24] W. E. Hagston and H. Ketterl, Phys. Rev. E **59**, 2699 (1999).

[25] F. D. A. Aarão Reis and D. F. Franceschini, Phys. Rev. E **61**, 3417 (2000); Y. Kim, D. K. Park, and J. M. Kim, J. Phys. A **27**, L533 (1994).

[26] F. D. A. Aarão Reis, Phys. Rev. E **70**, 031607 (2004).

[27] E. Marinari, A. Pagnani, and G. Parisi, J. Phys. A **33**, 8181 (2000); F. D. A. Aarão Reis, Phys. Rev. E **69**, 021610 (2004).

[28] F. D. A. Aarão Reis, Phys. Rev. E **72**, 032601 (2005).

[29] S.-C. Park, D. Kim, and J.-M. Park, Phys. Rev. E **65**, 015102(R) (2001).

[30] Z. Toroczkai, G. Korniss, S. Das Sarma, and R. K. P. Zia, Phys. Rev. E **62**, 276 (2000); F. Hivert, S. Nechaev, G. Oshanin, and O. Vasilyev, J. Stat. Phys. **126**, 243 (2007).